Civil and Sustainable Urban Engineering

Research Article
Volume 5(2), 2025, 195–212
https://doi.org/10.53623/csue.v5i2.867

Optimizing Geometric Alignment of High-Speed Railway in Hazard-Prone and Topographically Challenging Regions: A Case Study of the Bandung–Cirebon Corridor, Indonesia

Adya Aghastya, Aldi Wardana Yudha*

Construction and Railway Technology, Indonesia Railway Polytechnic, Jl. Tirta Raya, Pojok, Nambangan Lor, Kec. Manguharjo, Kota Madiun, Jawa Timur, 63129, Indonesia

*Correspondence: aldiwardana51@gmail.com

SUBMITTED: 24 October 2025; REVISED: 17 November 2025; ACCEPTED: 20 November 2025

ABSTRACT: The development of high-speed rail (HSR) infrastructure in Indonesia, particularly along the Bandung–Cirebon corridor, required precise geometric planning to ensure operational efficiency, safety, and long-term performance. This study aimed to design an optimized alignment for the Phase III segment between Ligung and Tengahtani by integrating engineering criteria with spatial and environmental constraints. A descriptive-analytic method was employed, combining field surveys, Digital Elevation Model Nasional (DEMNAS) data, and spatial planning documents, which were processed using Global Mapper and AutoCAD Civil 3D to generate alignment models, earthwork calculations, and spatial risk assessments. The proposed design featured five main horizontal curves with radii ranging from 2,500 to 12,000 meters and fourteen vertical curves with a constant 25,000-meter radius, meeting technical standards for a maximum operational speed of 350 km/h. Earthwork estimation yielded approximately 4.82 million m^3 of excavation and 47,208 m^3 of fill, while land acquisition requirements totaled around 1.83 million m^2, primarily affecting agricultural and residential zones. Spatial analysis identified 1.64 million m^2 of the proposed corridor as being located in moderate- to high-seismic-hazard zones, emphasizing the need for structural mitigation strategies and geotechnical monitoring. The findings highlighted the critical importance of integrating geometric design with topographical and hazard data in planning resilient HSR infrastructure. This study provided a replicable framework for railway alignment in complex terrain and supported sustainable transportation development in Indonesia's rapidly evolving intercity network.

KEYWORDS: Railway infrastructure planning; geometric alignment design; Indonesian high-speed railway; and earthwork analysis

1. Introduction

The rapid evolution of high-speed railway (HSR) networks transformed the landscape of intercity transportation, offering unparalleled travel speed, safety, and environmental sustainability. Unlike conventional rail systems, HSR services were specifically designed for

passenger transportation, operating on dedicated tracks with optimized geometrical alignment to support speeds exceeding 250 km/h [1]. In Indonesia, the adoption of HSR technology, as evidenced by the Jakarta–Bandung High-Speed Railway, catalyzed new demands for precise engineering design, particularly in geometric planning for future corridors such as the Bandung–Cirebon route.

One of the most crucial aspects of HSR infrastructure was geometric alignment planning, which determined the horizontal and vertical track configurations, transition curves, cant design, and station spacing. These elements directly impacted dynamic train performance, track wear, maintenance schedules, and overall passenger comfort [2,3]. Improper geometric design accelerated degradation due to high dynamic loads, posing risks to structural integrity and increasing lifecycle costs [4]. Therefore, geometric design had to not only meet engineering feasibility but also optimize performance under long-term operational conditions.

Advanced modeling methods were developed to analyze and forecast track geometry degradation. For instance, Monte Carlo simulations were employed to predict geometry deterioration and restoration cycles [5, 6], supporting maintenance planning and risk mitigation in aging infrastructure. Furthermore, forecasting methods based on heuristic models proved effective in projecting track aging processes, contributing to cost-effective lifecycle asset management [7]. These approaches were applied by European operators such as SNCF, illustrating the critical role of predictive models in sustaining HSR infrastructure [6].

Another key parameter in geometric planning was the strategic distribution of stations. High-speed rail required careful balancing between accessibility and express travel time. Overly frequent stops significantly degraded service efficiency, while overly distant stations reduced regional connectivity. Research suggested that multi-criteria optimization models, including two-layer approaches, supported rational station placement and enhanced corridor utility [8]. A study on the Xi'an–Chengdu HSR line demonstrated how station layout influenced train throughput and passenger satisfaction [9].

Operational optimization was also closely linked with geometric planning. Time-dependent demand patterns required flexible line planning strategies. Recent studies proposed game-theory-based frameworks, such as Stackelberg Game models, to integrate passenger flow behavior into scheduling and alignment strategies [10, 11]. These frameworks enabled more responsive infrastructure planning, particularly in corridors expected to serve fluctuating demand levels across time horizons.

From a structural perspective, the safety and stability of HSR tracks were essential considerations during both construction and long-term operation. Ground deformation, soil–structure interaction, and subgrade settlement needed to be evaluated through advanced geotechnical modeling. For example, 3D numerical models were used to simulate ballasted track responses under high-speed loads [12], while stability analyses of tunnel construction beneath HSR foundations revealed potential risks and mitigation strategies [13]. On-site monitoring during critical phases such as embankment formation and tunneling also provided empirical insights that complemented design simulations [14].

Despite technological advancements, significant challenges persisted, especially in mixed-use corridors where high-speed and lower-speed rail coexisted. Although Indonesia's HSR development currently excluded freight traffic, design standards still had to account for structural loading, trainset variations, and safety buffers [15]. Moreover, real-world infrastructure degradation such as track settlement, slab cracking, or interlayer defects

demanded robust quality control and adaptive geometric design [16, 17]. Recent machine learning approaches, such as PSO-SVM models, were introduced for defect detection in slab tracks, enabling proactive maintenance [11, 18].

Within the context of Bandung–Cirebon HSR Phase III—particularly the Ligung–Tengahtani section at KM 67+000 to KM 100+685.72—topographical variability, geological conditions, and urban expansion presented additional layers of complexity. In regions like West Java, environmental factors such as flood susceptibility and land instability necessitated geometric planning integrated with hazard assessment [19]. Urban sprawl and inadequate spatial regulation further complicated corridor planning, demanding a multidisciplinary approach that integrated transportation engineering, urban planning, and geotechnical risk management [20, 21].

This study advanced previous high-speed rail (HSR) alignment research by integrating geometric design, spatial land acquisition, and seismic hazard modeling into a single GIS-based optimization framework. Unlike prior studies that analyzed geometry or environmental suitability separately, this research applied a unified, multi-criteria approach tailored to Indonesian terrain and regulatory standards. The novelty lay in demonstrating how the integration of DEMNAS data, field survey validation, and spatial hazard mapping could produce a technically optimized and policy-aligned corridor for future HSR planning in Indonesia.

This study aimed to address these interconnected challenges by developing a comprehensive geometric alignment plan for the Ligung–Tengahtani section of the Bandung–Cirebon HSR corridor. The research focused on optimizing horizontal and vertical alignments, determining appropriate station spacing, and ensuring long-term track integrity under high-speed dynamic loads. In doing so, the study contributed to the broader goal of sustainable and resilient railway infrastructure in Indonesia, aligning with best practices from global HSR systems while addressing the unique characteristics of the local environment.

2. Methodology

The research methodology followed a structured sequence to evaluate the geometric planning of the Bandung–Cirebon High-Speed Railway Phase III (Ligung–Tengahtani). The process began with problem identification and data collection from both primary and secondary sources. Primary data were obtained through field surveys of the planned railway alignment, while secondary data included topographic maps and spatial planning documents (RTRW) from the provincial and local governments. These data were analyzed using engineering design software and GIS tools to generate geometric alignment models and spatial hazard maps. The overall workflow is illustrated in Figure 1. Figure 1 is a diagram illustrating the methodological sequence adopted in this study, from problem definition to final conclusions. It shows the integration of primary field data, secondary spatial data, geometric computation, and seismic analysis in developing a feasible high-speed rail alignment. Each stage produced specific outputs, such as geometric parameters, earthwork estimations, and earthquake-prone area mappings, which collectively informed the final route selection and design evaluation.

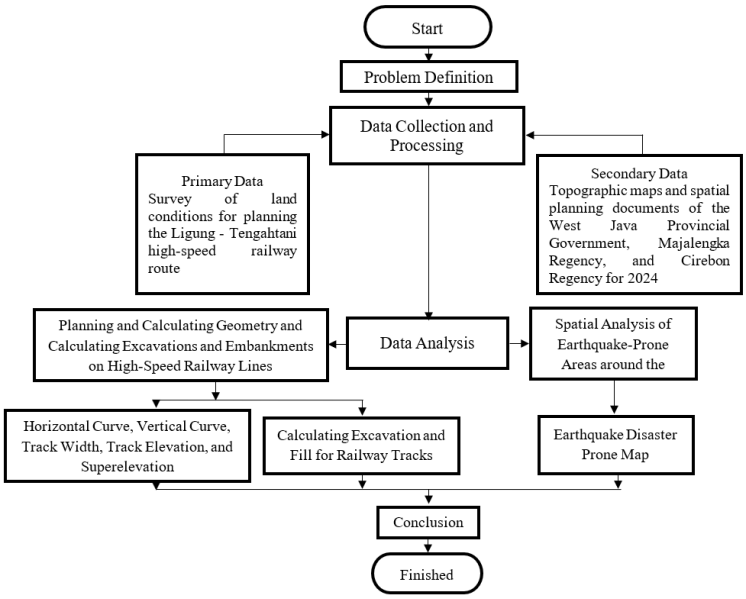

Figure 1. Research flow diagram for high-speed railway geometric planning.

2.1.Study design.

This study employed a descriptive-analytic observational approach to evaluate and design the geometric alignment of the High-Speed Railway (HSR) Line Bandung–Cirebon Phase III (Ligung–Tengahtani), covering STA KM 67+000 to KM 100+685.72. The methodology followed a systematic sequence, beginning with a route alignment review based on spatial planning policies, followed by detailed topographical analysis and geometric calculations. These procedures were intended to ensure that the alignment complied with local development plans, terrain conditions, and high-speed rail geometric standards.

2.2. Data sources and materials.

This study integrated both primary and secondary data to support the geometric design of the High-Speed Railway corridor. Spatial planning documents, including the Regional Spatial Plans (RTRW) of West Java Province, Majalengka Regency, and Cirebon Regency, provided the basis for initial corridor planning. Topographic data were obtained from the Digital Elevation Model Nasional (DEMNAS) with a 0.27 arc-second resolution (approximately 8.1 meters), sourced from Badan Informasi Geospasial (BIG), which served as the primary elevation reference. Field verification was conducted using sub-meter accuracy survey instruments to collect coordinate points along the proposed corridor, validating the terrain profile and overlaying it with digital data. Software tools supported data processing and design, including Global Mapper v24.0 for topographic extraction and geospatial analysis, and AutoCAD Civil 3D 2023 for geometric design, alignment modeling, slope analysis, and earthwork volume estimation. Similar approaches integrating DEM and GIS for rail route evaluation have been applied in alignment feasibility studies globally [22].

2.3. Field survey and data acquisition.

A field survey was conducted along strategic checkpoints of the Bandung–Cirebon Phase III corridor. Survey points were selected based on key terrain transitions, hydrological crossings, and land use sensitivity. The coordinates and elevations of each location were recorded with

real-time differential correction to ensure optimal accuracy. The survey was performed during dry weather conditions to minimize atmospheric interference and improve GPS signal reliability. Checkpoints were established at 500-meter intervals along the proposed corridor to provide consistent spatial representation of terrain variation, with additional points added at locations exhibiting elevation differences exceeding 5 meters or at critical features such as river crossings and steep slopes. For hazard mapping, classification thresholds followed national guidelines from BNPB, with low hazard defined as peak ground acceleration (PGA) <0.15g, moderate hazard 0.15–0.25g, and high hazard >0.25g, corresponding to Modified Mercalli Intensity levels V–VIII. These standardized criteria improved the reproducibility and comparability of the study.

2.4. Data processing and alignment modelling.

Following field data collection, elevation and spatial data were integrated in Global Mapper, where contours and slope layers were extracted and exported in compatible formats for modeling in AutoCAD Civil 3D. The geometric parameters analyzed included horizontal alignment, considering curve radii, transition curves, and tangent sections; vertical profile, including gradients and vertical curves to ensure compliance with high-speed rail standards (maximum 3.5‰ gradient and minimum vertical curve radius of 25,000 m for 350 km/h design speed); cross-sections and longitudinal sections generated every 250 meters to evaluate earthwork requirements and structural implications; and volume calculations, including cut and fill, for each segment to support preliminary construction planning. This integration of digital terrain modeling (DTM) and CAD-based alignment design is consistent with best practices in railway infrastructure planning [23].

2.5. Spatial analysis and route optimization.

Spatial analysis and route optimization were conducted using overlay techniques to align the proposed railway with land use zones, road networks, water bodies, and conservation areas, ensuring that environmentally sensitive or legally restricted areas were avoided. To evaluate the accuracy of DEMNAS, 45 ground control points were collected using differential GPS with sub-meter accuracy. Comparison of elevation data between DEMNAS and field measurements produced a Root Mean Square Error (RMSE) of 1.74 meters, confirming that DEMNAS was sufficiently accurate for geometric design and earthwork estimation at the preliminary HSR planning stage. This validation also provided a correction reference for slope and volume analyses, enhancing the reliability of subsequent geometric modeling [24].

3. Results and Discussion

Each technical component in this study was sequentially interconnected to ensure that the final alignment represented an optimal balance of engineering feasibility and environmental compliance. Route selection defined the feasible corridor based on spatial and regulatory constraints, while land acquisition analysis quantified the spatial feasibility of this corridor. Geometric alignment design subsequently refined the route to achieve technical efficiency within these spatial limits, and seismic hazard analysis validated the final alignment in terms of safety and resilience. This integrative approach ensured that every design decision contributed to a coherent and robust high-speed rail alignment.

3.1. Route determination.

The determination of the high-speed railway (HSR) route between Bandung and Cirebon in this study was based on the technical requirements of the Indonesian Ministry of Transportation Regulation No. 11/2012, ensuring conformity with national infrastructure planning standards. Route alignment analysis incorporated spatial planning documents from West Java Province, Majalengka Regency, and Cirebon Regency to ensure compatibility with existing development and minimize land-use conflicts. The selected alignment was designed to run parallel to the Cisumdawu Toll Road, simplifying construction logistics and reducing potential environmental and social disruptions. This study emphasized a balanced approach between technical feasibility and sustainability by integrating topographical surveys, land-use analysis, and socio-environmental considerations. High-speed rail projects, when integrated with spatial planning and supported by robust multicriteria analysis, were shown to enhance connectivity and promote regional growth. Previous studies also highlighted that HSR alignment planning should optimize land acquisition and environmental impact mitigation by aligning with existing corridors and minimizing slope constraints [25−27]. The integration of GIS-based tools into route selection further enhanced the ability to identify optimal alignments while reducing spatial conflicts and supporting environmental sensitivity [28−30]. In Indonesia, recent geometric design studies emphasized the need for alignment planning that conformed to national and international technical standards, particularly regarding curve radius, terrain constraints, and embankment strategies. At the preliminary stage, three alignment alternatives were evaluated: the northern route via Kadipaten–Ciwaringin, the central route along the Cisumdawu–Sumberjaya–Tengahtani axis, and the southern route through Rajagaluh–Palimanan. The central corridor was ultimately selected, as it reduced land acquisition in densely populated zones by approximately 18 percent, avoided high-slope areas exceeding 25° present in the southern alignment, ensured compliance with Ministry of Transportation Regulation No. 11/2012, and facilitated construction logistics by paralleling the Cisumdawu Toll Road [25, 31].

3.2. Land acquisition requirements.

Table 1 presents the land area required for the proposed high-speed rail alignment, categorized by land-use types based on field surveys and spatial analysis using ArcGIS. The total land required for the Bandung–Cirebon high-speed rail corridor was approximately 1.83 million square meters, as determined through spatial digitization and field validation. The calculation followed the requirements of the Indonesian Ministry of Transportation Regulation No. 7/2023, which mandated a clearance of 25 meters on each side of the centerline (as-track) of the proposed rail route. Agricultural areas dominated land acquisition, with paddy fields and plantations covering nearly 76% of the total corridor area. This finding underscored the importance of implementing fair compensation mechanisms and agricultural land conversion policies in accordance with local regulations.

Table 1. Land use area requirements.

No.	Land Use Type	Area (m^2)	Percentage (%)
1	Buildings	7.86	0.43
2	Plantation	163,854.16	8.95
3	Residential	274,028.61	14.97
4	Paddy Fields	1,236,977.95	67.57
5	Rivers	4,292.46	0.23

No.	Land Use Type	Area (m^2)	Percentage (%)
6	Fields	150,736.84	8.25
	Total	**1,829,897.88**	**100**

Figure 2 illustrates the proposed Phase III alignment, derived from GIS-based spatial analysis and overlaid on land-use data obtained from the West Java Provincial spatial planning database and DEMNAS topographic layers. A north arrow, scale bar, and legend were included to support spatial interpretation. The map identified major land-use categories intersected by the railway corridor, including agricultural, residential, plantation, and river zones, which were critical for land acquisition planning and environmental assessment. By integrating field survey data with GIS software, the study ensured more accurate planning and efficient land management. Together, Table 1 and Figure 2 highlighted the land-use impacts of the proposed railway alignment, providing essential information for identifying affected zones and minimizing social and environmental disruption.

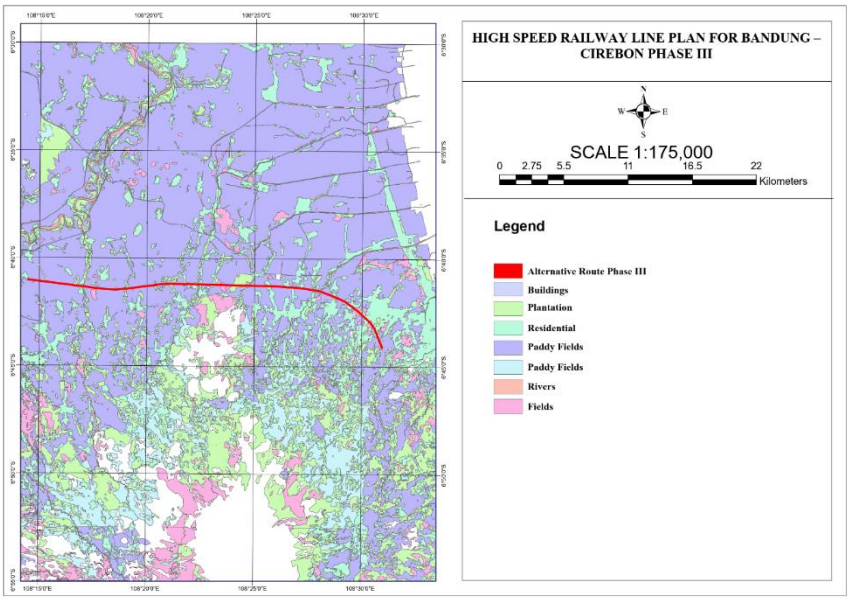

Figure 2. Proposed high speed railway alignment overlaid on land use zones, derived from GIS analysis.

Studies have shown that GIS-based methods not only improved spatial accuracy but also significantly enhanced land acquisition planning by identifying sensitive zones early in the design process [32]. Such integration facilitated a more informed and responsive decision-making process during large-scale infrastructure development. Furthermore, GIS-based spatial analysis proved effective in optimizing land acquisition strategies and detecting environmentally sensitive areas and disaster-prone zones [27, 33–34]. In similar cases, spatial decision support systems (SDSS) improved cost estimation for land compensation, construction feasibility, and socio-economic risk minimization [26, 35]. The spatial analysis indicated that approximately 15 percent of the affected land area consisted of residential and built-up zones, implying potential resettlement requirements. Early coordination with local governments was critical to establish compensation mechanisms and minimize social disruption. According to regional land valuation benchmarks, acquisition and resettlement costs could have increased project expenditure by 8–10 percent if not managed systematically. Integrating GIS-based social impact assessment in the early design phase helped prioritize alignment alternatives with lower displacement potential, improving both project feasibility and community acceptance.

3.3. Geometric alignment design.

The geometric alignment planning for the Bandung–Cirebon high-speed railway was carried out using contour data from Indonesia's DEMNAS (National DEM), which integrated various sources including IFSAR (5 m), TERRASAR-X (resampled to 5 m), and ALOS PALSAR (11.25 m), along with mass point data from the Indonesian Topographic Map (RBI) to enhance terrain detail accuracy. The railway geometry design complied with the Indonesian Ministry of Transportation Regulation No. 7/2022 and the Chinese technical standard TB 10621-2014, which are commonly adopted in high-speed railway projects in Asia. The maximum design speed was 400 km/h, while the operational speed was set at 350 km/h to ensure safety and prevent derailments. The track was designed as a double-track system with a standard gauge of 1435 mm, aligning with global high-speed rail best practices for speed and stability.

Recent research on railway geometric design in Indonesia emphasized that the combination of DEMNAS and high-resolution digital terrain models significantly enhanced the accuracy of route geometry planning, particularly in curved and hilly areas [25, 29]. The use of software such as AutoCAD Civil 3D and GIS-based topographic modeling contributed to optimizing vertical and horizontal alignments for safety and material efficiency [30]. Additionally, the selection of rail components, such as R60 rails, was validated to meet dynamic load requirements of EMU CR400AF trains at speeds up to 350 km/h with a safety factor of 1.7, supporting structural stability across variable terrains [31]. These design considerations also aligned with global practices for minimizing operational risks and improving long-term track durability under high-speed conditions.

3.3.1. Horizontal curve design.

Horizontal curve parameters such as minimum curve radius (R_{min}), transition length (L_s), and superelevation (h_r) were calculated using TB 10621-2014 standards. The minimum curve radius required varies depending on design speed and applied cant. For example, Curve 1 was designed for 350 km/h with a radius of 8000 m and a transition length of 470.5 m. Table 2 presents the detailed computation results and Figure 3 illustrates the geometric relationship among the main elements of the horizontal alignment, including the transition curve length (Ls), circular curve length (Lc), curve radius (Rc), deflection angle (Δ), and key points such as TS, SC, CS, and ST.

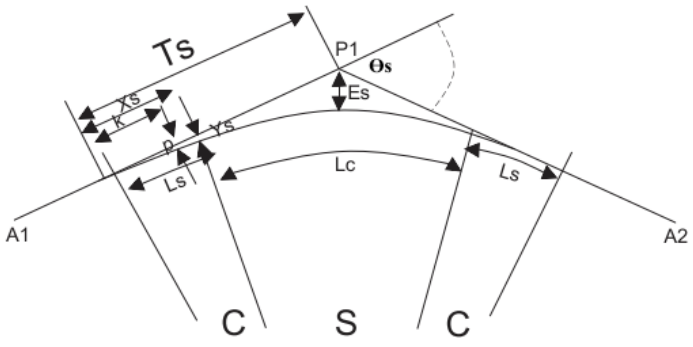

Figure 3. Geometric scheme of horizontal alignment for spiral–circular–spiral curve.

Table 2. Horizontal alignment parameters.

Alignmnet Horizontal		Curve 1	Curve 2	Curve 3	Curve 4	Curve 5
V (Km/h)		350	300	300	300	250
hr (mm)		175	175	175	175	175
hq (mm)		60	60	60	60	60
Rmin (m)		6151.064	4519.149	4519.149	4519.149	3138.298
Vmax Curve (km/jam)		397.628	486.993	486.993	397.628	222.281
Lmin Transition length (m)		188.172	470.430	470.430	470.430	392.025
hr (mm)		120.688	28.500	28.500	72.750	235.000
Plan R (m)		8000	12000	12000	8000	2500
Plan Ls (m)		470.5	300.0	300.0	470.5	270.0
A1	X	864740.414	869062.297	880251.815	882468.527	886923,927
	Y	9259259.327	9259535.761	9259386.234	9259149.248	9257017,628
P1	X	865207.752	869359.710	880551.635	882931.593	887606,216
	Y	9259209.546	9259575.058	9259375.900	9259068.916	9256399,877
A2	X	866746.869	871045.817	881825.439	886570.816	888080,224
	Y	9259224.648	9259663.872	9259253.069	9257327.830	9255740,250
αA-P1 (degrees)		96.080	82.473	91.974	99.842	132.158
αP1-P2 (degrees)		89.438	86.985	95.508	115.567	144.299
ΔPI-1 (degrees)		6.642	4.512	3.534	15.726	12.141
d (m)		469.982	299.998	299.998	469.982	920.399
Θs (derajat)		1.6857	0.7166	0.7166	1.6857	3.0955
Lc (m)		456.486	644.438	439.756	1724.131	259.482
Xs (m)		470.500	300.000	300.000	470.500	270.000
Ys (m)		4.612	1.250	1.250	4.612	4.860
p (m)		1.150	0.312	0.312	1.150	1.212
k (m)		235.124	149.923	149.923	235.124	134.918
Ts (m)		699.439	622.638	520.115	1340.099	400.918
Es (m)		14.611	9.619	6.020	77.089	15.317
Track Widening (mm)		10.679	7.158	7.158	10.679	33.916

Figure 3 illustrates the geometric relationship among the main elements of the horizontal alignment, including the transition curve length (Ls), circular curve length (Lc), curve radius (Rc), and deflection angle (Δ). The schematic also shows the key station points TS (tangent to spiral), SC (spiral to circular), CS (circular to spiral), and ST (spiral to tangent) that define the layout of the alignment curve. This figure provides a visual reference for understanding the alignment parameters used in the design analysis.The transition curve ensures smooth lateral acceleration changes, while the applied superelevation (cant) balances centrifugal forces. Superelevation values were calculated at four transition points per curve. Table 3 displays the calculated cant distribution for each curve.

Table 3. Superelevation distribution.

Superelevation	Curve 1	Curve 2	Curve 3	Curve 4	Curve 5
Plan Ls (m)	470	300	300	470	270
Lc (m)	457	644	440	1725	259
hr (mm)	120,688	60,458	60,458	120,688	128,800
Point 1 (mm)	30,172	15,115	15,115	30,172	32,200
Point 2 (mm)	60,344	30,229	30,229	60,344	64,400
Point 3 (mm)	90,516	45,344	45,344	90,516	96,600
Point 4 (mm)	120,688	60,458	60,458	120,688	128,800

The results indicated that the highest cant (128.8 mm) occurred at Curve 5, while the lowest was 60.46 mm at Curves 2 and 3. Accurate cant design was critical to maintain comfort and safety at high speeds, particularly in curves with tight radii. Improper superelevation in curves led to increased lateral acceleration and passenger discomfort, especially in overlapping zones between vertical and horizontal curves. Additionally, inadequate cant resulted in

increased rail wear and reduced structural lifespan of components due to unbalanced dynamic loads [36, 37]. Implementing appropriate superelevation distribution not only improved ride quality but also extended maintenance intervals, as demonstrated in optimized S-shaped and transition ramp models for high-speed tracks [38, 39]. Recent approaches suggested that integrating intelligent superelevation systems could allow real-time adjustments based on train type and speed, which is particularly beneficial in mixed-use corridors [40].

3.3.2. Vertical alignment design.

The geometric parameters were designed in accordance with the Indonesian Ministry of Transportation Regulation No. PM 7/2022 and the Chinese Technical Standard TB 10621-2014, which prescribed a minimum vertical curve radius of 25,000 meters and a maximum gradient of 3.5 per mille for trains operating at speeds up to 350 km/h. These standards ensured compliance with international high-speed rail safety and comfort requirements. In this study, parabolic vertical curves were applied to connect flat and inclined segments, minimizing vertical acceleration and ensuring smooth grade transitions along undulating terrain. A total of fourteen vertical curves were incorporated, reflecting the highly variable topography in the Majalengka–Cirebon corridor. Table 4 presented the computed parameters of each vertical curve, while Figure 4 illustrated the geometric configuration of the vertical alignment.

Table 4. Vertical alignment parameters.

Alignment Vertical	Curve 1	Curve 2	Curve 3	Curve 4	Curve 5	Curve 6	Curve 7
Rv	25000	25000	25000	25000	25000	25000	25000
Plan V	350	350	350	350	350	350	350
g1 (%)	0.180	0.360	0.150	0.040	0.240	0	0.130
g2 (%)	0.360	0.150	0.040	0.240	0.000	0.130	-0.080
A (%)	0.180	0.210	0.110	0.200	0.240	0.130	0.210
Lv (m)	4500	5250	2750	5000	6000	3250	5250
Ev (m)	1.013	1.378	0.378	1.250	1.800	0.528	1.378
lp	2390	2765	1515	2640	3140	1765	2765
Alignment Vertical	**Curve 8**	**Curve 9**	**Curve 10**	**Curve 11**	**Curve 12**	**Curve 13**	**Curve 14**
Rv	25000	25000	25000	25000	25000	25000	25000
Plan V	350	350	350	350	350	350	350
g1 (%)	-0.080	0.240	-0.220	-0.370	-0.280	0	0.060
g2 (%)	0.240	-0.220	-0.370	-0.280	0.000	-0.100	0.210
A (%)	0.320	0.460	0.150	0.090	0.280	0.100	0.150
Lv (m)	8000	11500	3750	2250	7000	2500	3750
Ev (m)	3.200	6.613	0.703	0.253	2.450	0.313	0.703
lp	4140	5890	2015	1265	3640	1390	2015

Figure 4 illustrates the geometric configuration of the vertical alignment. The schematic depicts the relationships among key parameters, including the initial and final gradients (g_1 and g_2), the vertical curve length (Lv), the algebraic difference in grade (A), the radius of curvature (Rv), and the elevation offset (Ev). This configuration demonstrates how parabolic curves were applied to provide smooth grade transitions between consecutive track segments. This design approach ensured a continuous and smooth profile, accommodating high-speed operations and

variable terrain. Vertical alignment played a pivotal role in minimizing energy consumption and reducing wear on mechanical components [41]. Improperly matched vertical-horizontal overlaps could intensify vehicle vibrations, particularly in sections dominated by convex or concave profiles, potentially compromising operational safety. Simulation models indicated that the dynamic response of high-speed trains was highly sensitive to vertical accelerations at transition points, highlighting the need for careful calibration of vertical curve radii [42, 43].

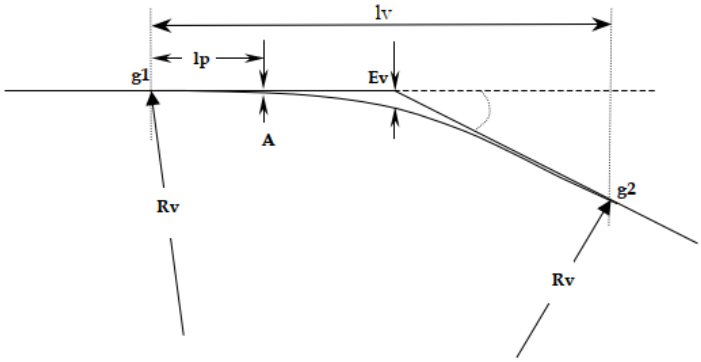

Figure 4. Geometric scheme of vertical alignment.

3.4.Earthwork volume calculation.

Earthwork volume for the high-speed railway track was calculated using cross-sectional data at regular 500-meter intervals, applying the average-end-area method. This method is widely recognized for its reliability in large-scale linear infrastructure projects, where terrain variation must be systematically considered [44]. The calculations were verified against topographic corrections and field measurements from cross-section profiles. As shown in Table 5, the cumulative earthwork totals reached 4,822,112.64 m³ for excavation and 47,208.29 m³ for embankment, reflecting the predominance of cut sections along the corridor. Accurate estimation of cut-and-fill volumes is essential to optimize construction costs, minimize environmental impact, and improve planning efficiency. Integrating Digital Terrain Models (DTMs) and GIS-based methods further enhanced the precision of volume predictions in complex terrain, as highlighted in recent studies [45]. Table 5 shows Earthwork volume from station 97+000 to 100+685.72.

Table 5. Earthwork volume from station 97+000 to 100+685.72.

Station	Cut Area (m^2)	Cut Volume (m^3)	Fill Area (m^2)	Fill Volume (m^3)	Cumulative Cut Volume (m^3)	Cumulative Cut Volume (m^3)
67+000	…	…	…	…	…	…
…	…	…	…	…	…	…
97+500	18.20	4,550.31	31.46	7,866,24	4,378,247.54	34,051.51
98+000	18.20	4,550.31	26.31	6,578,40	4,382,797.85	40,629.90
98+500	46.38	11,594.47	26.31	6,578,39	4,394,392.32	47,208.29
99+000	49.01	23,848.15	-	-	4,418,240.46	47,208.29
99+500	234.58	70,898.52	-	-	4,489,138.98	47,208.29
100+000	231.38	116,490.86	-	-	4,605,629.84	47,208.29
100+500	379.84	152,805.60	-	-	4,758,435.45	47,208.29
100+685,72	305.88	63,677.20	-	-	4,822,112.64	47,208.29

Although excavation accounted for the majority of earthwork, several optimization strategies could reduce both cost and environmental impact. These include reusing cut material for embankment construction, balancing cut-and-fill volumes within sub-segments, and applying slope-terrace techniques to stabilize steep terrain. Implementing such measures can reduce hauling distances and associated carbon emissions by an estimated 12–18%, as demonstrated in comparable high-speed rail projects [46].

3.5.Spatial analysis of earthquake-prone areas.

This integrated spatial analysis provided a robust basis for identifying critical segments where structural countermeasures were necessary, such as embankment reinforcement, flexible track systems, or seismic isolation bearings. Areas with high slope inclinations intersecting zones of elevated MMI levels were found to significantly increase the probability of earthquake-induced landslides, posing major threats to track stability and safety. Regions prone to liquefaction, particularly those underlain by loose alluvial deposits, required preemptive engineering treatments such as ground improvement or foundation isolation. Recent research has emphasized the importance of coupling seismic hazard maps with site-specific geotechnical data to more accurately quantify risk zones along railway alignments [47].

The application of GIS-based multi-criteria evaluation (MCE) frameworks enabled more precise spatial weighting of risk parameters, enhancing decision-making during the alignment optimization and design phases [48]. This approach was particularly relevant in tectonically active regions such as Java, where shallow crustal earthquakes occur frequently and produce nonlinear site responses due to local soil conditions [49]. Additionally, probabilistic seismic hazard models combined with terrain analysis have been widely applied in infrastructure planning to identify and prioritize mitigation strategies for high-risk segments, including early warning systems and alignment re-routing.

Figure 5 presents the seismic hazard map, constructed from historical earthquake records, geological data, and seismic modeling. Modified Mercalli Intensity (MMI) values were classified into moderate (V–VI), high (VII–VIII), and very high (>VIII) categories. Simultaneously, slope data derived from a Digital Elevation Model (DEM) was processed in ArcGIS to produce inclination maps categorized as flat (<15°), moderate (15°–30°), and steep (>30°). These datasets were integrated using a weighted overlay technique to classify combined risk into low, medium, and high zones. This classification is vital for land use regulation, earthquake-resilient infrastructure planning, and emergency response strategies. For alignment segments located in high-risk seismic zones (MMI VII–VIII with slopes > 30°), engineering mitigation measures are essential. Recommended strategies include pile-supported embankments, deep-soil-mixing ground improvement, flexible pier systems, and installation of seismic isolation bearings. Continuous geotechnical monitoring and early-warning instrumentation should be implemented to ensure long-term operational safety.

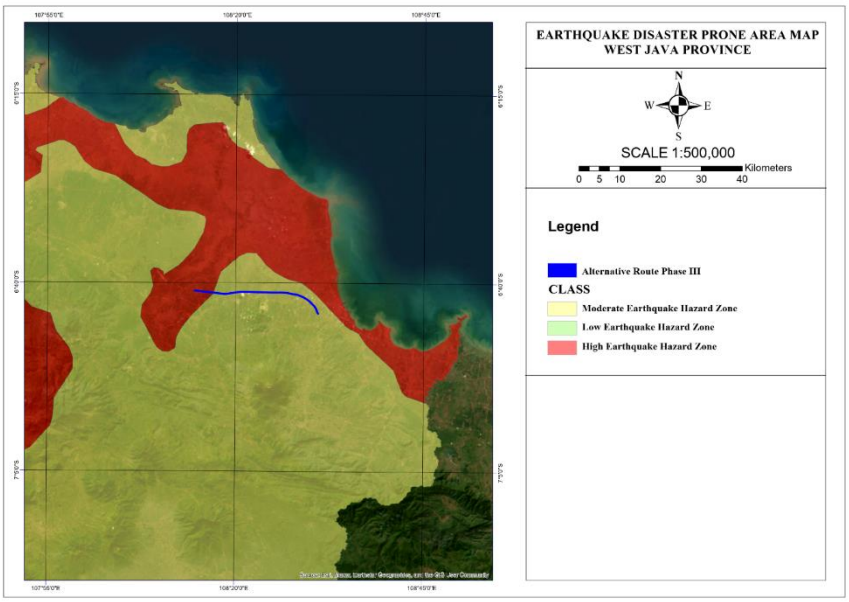

Figure 5. Spatial overlay showing detailed intersection of the proposed HSR alignment with existing land use categories.

Table 6 shows the total land area within each hazard category crossed by the proposed railway alignment. Approximately 1,398,494.45 m² of the corridor fell within the moderate-risk zone, while 243,811.26 m² was located in the high-risk zone. These findings reinforced the importance of considering seismic risk as a critical parameter in route planning and design. Previous studies highlighted that combining liquefaction potential, ground shaking, and slope instability provides a more comprehensive assessment of seismic hazard impacts for linear infrastructure such as railways [49, 50]. GIS-based seismic risk models were successfully applied to assess regional vulnerability and optimize route alignment in hazard-prone areas [51–53]. Additionally, probabilistic and machine learning approaches emerged as robust tools for mapping complex multi-hazard zones, offering higher spatial resolution for infrastructure-specific risk evaluation [54].

For segments intersecting high-seismic-intensity zones (MMI VII–VIII), several engineering countermeasures were recommended. These included the use of pile-supported embankments on soft or liquefiable soils, application of seismic isolation bearings in bridge structures, and adoption of ballastless slab track systems with flexible joints. All structural components in these zones were designed in accordance with SNI 1726:2019 for earthquake-resistant design. Continuous geotechnical monitoring, slope stabilization, and early warning systems were also advised to enhance operational safety throughout the service life of the railway.

Table 6. Area of traces in earthquake-prone areas.

Hazard Zone Classification	Total (m^2)
Moderate Earthquake Hazard Zone	1,398,494.45
High Earthquake Hazard Zone	243,811.26
Total	**1,642,305.71**

4. Conclusions

This study provides a comprehensive analysis and geometric planning for the Bandung–Cirebon High-Speed Railway (HSR) Phase III, particularly in the Ligung–Tengahtani segment. By combining GIS-based spatial analysis, field surveys, and engineering modeling, the research demonstrates how technical feasibility, environmental concerns, and spatial policies must be integrated in high-speed rail development. The total land required for this project is approximately 1.83 million square meters, dominated by agricultural lands such as paddy fields

and plantations, along with residential and built-up areas. This significant land use underscores the importance of careful acquisition planning to minimize social disruption and support sustainable regional growth. From a design perspective, the horizontal alignment consists of five main curves with radii between 2,500 and 12,000 meters, supporting a maximum operational speed of 350 kilometers per hour. The vertical alignment features 14 curves with a radius of 25,000 meters and maximum allowable gradients of 30 per mille, ensuring safe and smooth transitions along varied terrain. Earthwork volume estimation, using AutoCAD Civil 3D and validated by manual calculations at 500-meter intervals, resulted in a total excavation volume of approximately 4.82 million cubic meters and a fill volume of around 47,208 cubic meters. These calculations are essential for budgeting, construction planning, and environmental impact assessment. Spatial hazard analysis revealed that around 1.64 million square meters of the proposed railway corridor falls within earthquake-prone areas, classified as moderate to high risk. This finding emphasizes the need for mitigation measures such as early warning systems and strengthened structural designs in those zones. By integrating terrain data, alignment modeling, and multi-layer spatial analysis, this study provides a practical framework for planning high-speed rail infrastructure in complex environments. Future research should explore the long-term performance of the proposed design under seismic and environmental stress, as well as the socio-economic effects of large-scale land acquisition on local communities. The outcomes of this research offer actionable insights for transportation authorities and planners to improve land acquisition efficiency, embed seismic risk considerations in early design stages, and promote sustainable infrastructure development. The methodological framework proposed herein can serve as a reference model for future Indonesian high-speed rail projects facing similar geotechnical and spatial challenges.

Acknowledgments

The authors would like to extend their sincere appreciation to the Department of Construction and Railway Technology, Indonesia Railway Polytechnic (PPI Madiun), for their valuable support, technical guidance, and institutional facilitation throughout the course of this research project.

Competing Interest

The authors confirm that they have no financial interests or personal relationships that could have influenced the research or outcomes presented in this paper.

Author Contribution

Aldi Wardana Yudha was responsible for the conceptualization, methodology, data collection, data analysis, and preparation of the original manuscript draft. Adya Aghastya contributed to the conceptualization, provided supervision, and performed critical review and editing of the manuscript, offering both substantive and editorial feedback throughout the writing process.

Data Availability

The datasets used and analyzed in this study include publicly available spatial and topographic data obtained from the Digital Elevation Model Nasional (DEMNAS) provided by Badan Informasi Geospasial (BIG) and regional spatial planning documents (RTRW) from provincial

and local governments. Primary field survey data supporting this study are available from the corresponding author upon reasonable request.

References

[1] Li, F.; Wang, K.; Li, X.; Zhang, H.; Li, Y. (2022). The Evaluation and Key-Factor Identification of the Influence of Tourism on the Soil of Mount Tai. *Sustainability*, *14*, 13929. https://doi.org/10.3390/su142113929.

[2] Wang, L.; Jia, L.; Qin, Y.; Xu, J.; Mo, W. (2011). A two-layer optimization model for high-speed railway line planning. *Journal of Zhejiang University – SCIENCE A*, *12*, 902–912. https://doi.org/10.1631/jzus.A11GT016.

[3] Zhao, S.; Wu, R.; Shi, F. (2021). A line planning approach for high-speed railway network with time-varying demand. *Computers & Industrial Engineering*, *160*, 107547. https://doi.org/10.1016/j.cie.2021.107547.

[4] Varandas, J.N.; Paixão, A.; Tijera, Á.; Crespo-Chacón, I.; Estaire, J.; Fortunato, E. (2025). Dynamic response of ballasted High-Speed Railways: insights from experimental measurements and 3D nonlinear numerical modelling. *Transportation Geotechnics*, *52*, 101549. https://doi.org/10.1016/j.trgeo.2025.101549.

[5] Quiroga, L.M.; Schnieder, E. (2012). Monte Carlo simulation of railway track geometry deterioration and restoration. *Proceedings of the Institution of Mechanical Engineers, Part O: Journal of Risk and Reliability*, *226*, 274–282. https://doi.org/10.1177/1748006X11418422.

[6] Bris, R.; Soares, C.G.; Martorell, S. (2010). Reliability, Risk and Safety. CRC Press: London, UK. https://doi.org/10.1201/9780203859759.

[7] Quiroga, L.; Schnieder, E. (2012). Heuristic Forecasting of Geometry Deterioration of High Speed Railway Tracks. In: *Proceedings*, pp. 609–616. https://doi.org/10.1007/978-3-642-27579-1_78.

[8] Shi, Y. (2014). Research on the Layout Method and Evaluation Model of High-Speed Railway Stations: A Case Study of Optimizing the Layout Scheme on Xi'an-Chengdu High-Speed Railway Stations. *Challenges and Advances in Sustainable Transportation Systems*, 397–403. https://doi.org/10.1061/9780784413364.049.

[9] Zhou, W.; Li, X.; Shi, X. (2023). Joint Optimization of Time-Dependent Line Planning and Differential Pricing with Passenger Train Choice in High-Speed Railway Networks. *Mathematics*, *11*, 1290. https://doi.org/10.3390/math11061290.

[10] Kurhan, M.; Fischer, S.; Tiutkin, O.; Kurhan, D.; Hmelevska, N. (2024). Development of High-Speed Railway Network in Europe: A Case Study of Ukraine. *Periodica Polytechnica Transportation Engineering*, *52*, 151–158. https://doi.org/10.3311/PPtr.23464.

[11] Song, C.; Guo, Y; Li, S.; Chen, X.; Liu, X. (2024). Track Geometry Data-Driven Interlayer Defect Detection of High-Speed Rail Slab Track Based on PSO-SVM Model. *CICTP 2024* ASCE, 1378–1388. https://doi.org/10.1061/9780784485484.131.

[12] Fei, Z. (2022). Stability Analysis of Construction Process of New Tunnel Passing through High-speed Railway Foundation. *Journal of Railway Engineering Society*, *39*, 53–58. https://doi.org/10.1007/S13238-016-0264-7.

[13] Jinxing, L. (2021). Research on the Influence of Furong Town Station Connecting Line Project on Construction in Progress. *Journal of Railway Engineering Society*, *38*, 42–46. https://doi.org/10.1007/S13238-016-0264-7.

[14] Suwargana, H.; Zakaria, Z.; Muslim, D.; Haryanto, I.; Wahyudi, E. J.; Rohaendi, N. (2023). Gravity Modeling to Understand the Subsurface Geology of the Central Part of West Bandung Regency (Citatah Karst Area, Cipatat-Padalarang). *Trends in Sciences*, *20*, 6522. https://doi.org/10.48048/tis.2023.6522.

[15] Koglin, L.T. (2018). High-speed rail planning, policy, and engineering. Volume IV, Trends and advanced concepts in high-speed rail. Momentum Press: New York, USA.

[16] Cai, C.; Tian, S.; Shi, Y.; Chen, Y.; Li, X. (2024). Influencing Factors Analysis in Railway Engineering Technological Innovation under Complex and Difficult Areas: A System Dynamics Approach. *Mathematics*, *12*, 2040. https://doi.org/10.3390/math12132040.
[17] Sun, L.; Seyedkazemi, M.; Nguyen, C.C.; Zhang, J. (2023). Dynamics of Train–Track–Subway System Interaction—A Review. *Machines*, *13*, 1013. https://doi.org/10.3390/machines13111013.
[18] Cai, X.; Tang, X.; Pan, S.; Wang, Y.; Yan, H.; Ren, Y.; Chen, N.; Hou, Y. (2024). Intelligent recognition of defects in high-speed railway slab track with limited dataset. *Computer-Aided Civil and Infrastructure Engineering*, *39*, 911–928. https://doi.org/10.1111/mice.13109.
[19] Inaba, K.; Tanigawa, H.; Naito, H. (2024). Improvement of impact acoustic inspection for high-speed railway track slabs using time–frequency analysis and non-defective machine learning. *NDT & E International*, *145*, 103125. https://doi.org/10.1016/j.ndteint.2024.103125.
[20] Guo, G.; Cui, X.; Du, B. (2021). Random-Forest Machine Learning Approach for High-Speed Railway Track Slab Deformation Identification Using Track-Side Vibration Monitoring. *Applied Sciences*, *11*, 4756. https://doi.org/10.3390/app11114756.
[21] Sresakoolchai, J.; Kaewunruen, S. (2022). Railway defect detection based on track geometry using supervised and unsupervised machine learning. *Structural Health Monitoring*, *21*, 1757–1767. https://doi.org/10.1177/14759217211044492.
[22] Singh, M.P.; Singh, S.; Singh, P. (2024). Multi-criteria Decision Analysis for Route Alignment Planning Using Geographical Information System (GIS) and Analytical Hierarchy Process (AHP). *Chinese Journal of Urban and Environmental Studies*, *12*. https://doi.org/10.1142/S2345748124500064.
[23] Krischler, J.; Mellenthin Filardo, M.; Koch, C. (2022). GIS and BIM Integration Approaches for Early Railway Planning Phases, 2022 European Conference on Computing in Construction. https://doi.org/10.35490/EC3.2022.200.
[24] Song, T.; Pu, H.; Schonfeld, P.; Zhang, H.; Li, W.; Peng, X.; et al. (2021). GIS-based multi-criteria railway design with spatial environmental considerations. *Applied Geography*, *131*, 102449. https://doi.org/10.1016/j.apgeog.2021.102449.
[25] Aghastya, A.; Wardana, A.; Adi, W. T.; Imron, N. A.; Wirawan, W. A. (2023). Geometry Design of Railway Track for High-Speed Railways Bandung-Cirebon KM 00+000 - KM 33+850. *Journal of Railway Transportation and Technology*, *2*, 34–45. https://doi.org/10.37367/JRTT.V2I2.29.
[26] Kim, H.Y.; Wunneburger, D.; Neuman, M.; An, S.Y. (2014). Optimizing high-speed rail routes using a Spatial Decision Support System (SDSS): the Texas Urban Triangle (TUT) case. *Journal of Transport Geography*, *34*, 194–201. https://doi.org/10.1016/j.jtrangeo.2013.11.014.
[27] Suriadilaga, M.; Aghastya, A.; Danartini, R.S. (2024). Selection of The Cirebon-Semarang High Speed Railway Phase I (Cirebon-Brebes) Using ArcGIS 10.8. *Sainstech Nusantara*, *1*, 53–62. https://doi.org/10.71225/jstn.v1i2.49.
[28] Qiu, D.; Du, M.; Lu, S.; Shi, R. (2009). High-speed railway location design using GIS. In: *2009 IEEE International Geoscience and Remote Sensing Symposium*, IEEE, pp. II-650–II-653. https://doi.org/10.1109/IGARSS.2009.5418170.
[29] Purwaamijaya, I.M. (2019). Railway geometric design based on satellite imagery and digital terrain model. *Journal of Physics: Conference Series*, *1280*, 022030. https://doi.org/10.1088/1742-6596/1280/2/022030.
[30] Engelhardt, J. (2022). Planned spatial arrangement of high-speed railway lines in Poland. *Transportation Overview – Przegląd Komunikacyjny*, pp. 9–21. https://doi.org/10.35117/A_ENG_22_11_02.
[31] Dermawan, S.A.; Widyaningsih, N. (2024). Evaluation of the Strength Of R60 Type Rails Against Loading High-Speed Trains. *Journal of Social Research*, *3*, 1158–1171. https://doi.org/10.55324/JOSR.V3I5.2020.

[32] Liu, Y.-S.; Wang, J.-Y.; Guo, L.-Y. (2006). GIS-Based Assessment of Land Suitability for Optimal Allocation in the Qinling Mountains, China. *Pedosphere*, *16*, 579–586. https://doi.org/10.1016/S1002-0160(06)60091-X.

[33] Aleksandrowicz, S.; Turlej, K.; Lewiński, S.; Bochenek, Z. (2014). Change Detection Algorithm for the Production of Land Cover Change Maps over the European Union Countries. *Remote Sensing*, *6*, 5976-5994. https://doi.org/10.3390/rs6075976.

[34] Purba, A.; Nakamura, F.; Dwsbu, C.N.; Jafri, M.; Pratomo, P. (2017). A current review of high speed railways experiences in Asia and Europe. *AIP Conference Proceedings*, *1903,* 060004. https://doi.org/10.1063/1.5011558.

[35] Setiawan, A.; Hamka, H.; Ridwan, W.; Salsabila, F.; Zahidi, M.S. (2024). Indonesia's Strategic Interest in High-Speed Rail Cooperation with China: Analyzing the Jakarta-Bandung Project Under Jokowi's Infrastructure Vision. *Global International Journal of Innovative Research*, *2*, 2834–2851. https://doi.org/10.59613/global.v2i12.366.

[36] Shi, J.; Ma, D.; Gao, Y. (2021). Interaction Dynamic Response of a High-Speed Train Moving Over Curved Bridges with Deficient or Surplus Superelevation. *International Journal of Structural Stability and Dynamics*, *21*, 2150103. https://doi.org/10.1142/S0219455421501030.

[37] Beltiukov, V.P.; Andreev, A.V. (2021). Considering various conditions during determination of railway curve superelevation. *IOP Conference Series: Materials Science and Engineering*, *1151*, 012019. https://doi.org/10.1088/1757-899X/1151/1/012019.

[38] Torbic, D.J.; Donnell, E.T.; Brennan, S.N.; Brown, A.; O'Laughlin, M.K.; Bauer, K.M. (2014). Superelevation Design for Sharp Horizontal Curves on Steep Grades. *Transportation Research Record: Journal of the Transportation Research Board*, *2436*, 81–91. https://doi.org/10.3141/2436-09.

[39] Fan, X.; Li, B.; Zhang, Y.; Du, G.; Liu, H. (2021). Dynamic influence of the plane curve radius on vertical-circular overlapping lines of high-speed railway. *E3S Web of Conferences*, *248*, 03033. https://doi.org/10.1051/e3sconf/202124803033.

[40] Lin, P.; Liu, F.; Zhang, H. (2007). Intelligent System of Outer Rail Superelevation on Curve and its Key Technologies. In: *International Conference on Transportation Engineering*, ASCE, pp. 1106–1110. https://doi.org/10.1061/40932(246)182.

[41] Um, J.H.; Choi, I.Y.; Yang, S.C.; Kim, M.C. (2011). Optimization of alignment considering ride comfort for superimposition of vertical and horizontal curves. *Proceedings of the Institution of Mechanical Engineers, Part F: Journal of Rail and Rapid Transit*, *225*, 649–662. https://doi.org/10.1177/0954409710397641.

[42] Zhao, Y.; Wu, Y.; Zhao, M.; Xiang, Z.; Zhi, J.; Xu, B. (2023). Design and Evaluation of the Internal Space Layout of High-Speed Health Trains Based on Improved Systematic Layout Planning. *J, 6*, 361-383. https://doi.org/10.3390/j6030025.

[43] Liao, B.; Luo, Y. (2022). Influence of alignments of guide curves on the passing performance of railway turnout diverging route. *Vehicle System Dynamics*, *60*, 617–632. https://doi.org/10.1080/00423114.2020.1827152.

[44] Mohamed, A. (2019). Volume Calculation of Irregular Object Using Multiple Software Packages. *Journal of Al-Azhar University Engineering Sector*, *14*, 75–86. https://doi.org/10.21608/auej.2019.28507.

[45] Vasic, M.; Janić, N.; Đukanović, M.; Grujovic, G.; Dragomir. (2015). Earthwork Volume Calculation from Digital Terrain Models. *Journal of Industrial Design and Engineering Graphics*, *10*, 27–30.

[46] Shen, Q.; Pan, Y.; Feng, Y. (2023). The impacts of high-speed railway on environmental sustainability: quasi-experimental evidence from China. *Humanities and Social Sciences Communications*, *10*, 719. https://doi.org/10.1057/s41599-023-02135-6.

[47] Weng, M.-C.; Lin, M.-L.; Lo, C.-M.; Lin, H.-H.; Lin, C.-H.; Lu, J.-H.; et al. (2019). Evaluating failure mechanisms of dip slope using a multiscale investigation and discrete element modelling. *Engineering Geology*, *263*, 105303. https://doi.org/10.1016/j.enggeo.2019.105303.

[48] Hajimirzajan, A.; Kazemian, M.; Fischer, S. (2025). A Fuzzy Framework for Assessing and Prioritizing Railway Infrastructure Retrofitting Against Seismic Hazards – A Case Study. *Acta Polytechnica Hungarica*, *22*, 263–286. https://doi.org/10.12700/APH.22.4.2025.4.16.

[49] Zhang, M.; Seyler, B. C.; Di, B.; Wang, Y.; Tang, Y. (2021). Impact of earthquakes on natural area-driven tourism: Case study of China's Jiuzhaigou National Scenic Spot. *International Journal of Disaster Risk Reduction*, *58*, 102216. https://doi.org/10.1016/j.ijdrr.2021.102216.

[50] Farahani, S.; Shojaeian, A.; Behnam, B.; Roohi, M. (2023). Probabilistic Seismic Multi-hazard Risk and Restoration Modeling for Resilience-informed Decision Making in Railway Networks. *Sustainable and Resilient Infrastructure*, *8*, 470–491. https://doi.org/10.1080/23789689.2023.2170090.

[51] Barani, S.; Ferretti, G.; Scafidi, D. (2023). Evaluation of liquefaction triggering potential in Italy: a seismic-hazard-based approach. *Natural Hazards and Earth System Sciences*, *23*, 1685–1698. https://doi.org/10.5194/nhess-23-1685-2023.

[52] Debnatha, R.; Das, R.; Kumar, R.; Saha, R. (2024). Seismic hazard assessment of Agartala agglomeration based on 1D nonlinear ground response analysis and empirically derived liquefaction susceptibility. *Acta Geophysica*, *73*, 2181–2215. https://doi.org/10.1007/s11600-024-01502-4.

[53] Maneerat, P.; Rungskunroch, P.; Persaud, P. (2024). Seismic hazard analysis and financial impact assessment of railway infrastructure in the US West Coast: A machine learning approach. *PLOS ONE*, *19*, e0308255. https://doi.org/10.1371/journal.pone.0308255.

[54] Spacagna, R.L.; Cesarano, M.; Fabozzi, S.; Peronace, E.; Porchia, A.; Romagnoli, G.; et al. (2021). Geostatistical approach for multi-scale seismic liquefaction risk assessment. *EGU General Assembly 2021*. https://doi.org/10.5194/egusphere-egu21-12789.